

Article

# Synergistic Effect of MoS<sub>2</sub> and SiO<sub>2</sub> Nanoparticles as Lubricant Additives for Magnesium Alloy–Steel Contacts

Hongmei Xie <sup>1</sup>, Bin Jiang <sup>2,3,\*</sup>, Xingyu Hu <sup>4</sup>, Cheng Peng <sup>1,\*</sup>, Hongli Guo <sup>1</sup> and Fusheng Pan <sup>2,3</sup>

<sup>1</sup> College of Mechanical and Electrical Engineering, Yangtze Normal University, Chongqing 408100, China; xiehongmei@yznu.cn (H.X.); guohongli1211@163.com (H.G.)

<sup>2</sup> College of Materials Science and Engineering, National Engineering Research Center for Magnesium Alloys, Chongqing University, Chongqing 400044, China; fspan@cqu.edu.cn

<sup>3</sup> Chongqing Academy of Science and Technology, Chongqing 401123, China

<sup>4</sup> College of Materials Science and Engineering, Fudan University, Shanghai 200433, China; 16307110487@fudan.edu.cn

\* Correspondence: jiangbinrong@cqu.edu.cn (B.J.); 20090008@yznu.cn (C.P.); Tel./Fax: +86-023-6511-1140 (B.J.)

Academic Editor: Eva Pellicer

Received: 6 May 2017; Accepted: 15 June 2017; Published: 23 June 2017

**Abstract:** The tribological performances of the SiO<sub>2</sub>/MoS<sub>2</sub> hybrids as lubricant additives were explored by a reciprocating ball-on-flat tribometer for AZ31 magnesium alloy / AISI 52100 bearing steel pairs. The results demonstrated that the introduction of SiO<sub>2</sub>/MoS<sub>2</sub> hybrids into the base oil exhibited a significant reduction in the friction coefficient and wear volume as well as an increase in load bearing capacity, which was better than the testing results of the SiO<sub>2</sub> or MoS<sub>2</sub> nanolubricants. Specifically, the addition of 0.1 wt % nano-SiO<sub>2</sub> mixed with 1.0 wt % nano-MoS<sub>2</sub> into the base oil reduced the friction coefficient by 21.8% and the wear volume by 8.6% compared to the 1.0 wt % MoS<sub>2</sub> nanolubricants. The excellent lubrication behaviors of the SiO<sub>2</sub>/MoS<sub>2</sub> hybrid nanolubricants can be explained by the micro-cooperation of different nanoparticles with disparate morphology and lubrication mechanisms.

**Keywords:** SiO<sub>2</sub>/MoS<sub>2</sub> hybrids; lubricant additive; magnesium alloy; tribological properties

## 1. Introduction

Magnesium and its alloys exhibit many desirable intrinsic properties, such as low density (1.35–1.85 g/cm<sup>3</sup>), high specific strength and stiffness, excellent electromagnetic shielding characteristics, and abundant resources [1–4]. These favorable performances can be attributed specifically to the aspect of weight savings in design and construction for the automotive industry, mobile phones, aerospace components, and computers [5–7]. Especially, wrought Mg alloys, such as extruded profiles, rolled sheets, and forgings, possess better mechanical properties as compared to cast Mg alloys due to the ultrafine grain and the homogeneous distribution of the chemical composition after the plastic deformation [8]. However, the high friction and pick up of work material to the tool surfaces are inevitable issues in the cold forming process for magnesium alloys [9].

Controlling friction by lubrication is important in metal forming not only for reducing energy consumption but also for enhancing the surface quality of the formed components and the forming limitations [10]. Nonetheless, so far few lubricants are exclusively used for the forming process of Mg alloy, and in some cases, the forming lubricants used for Al alloy forming are casually used and the consequences are not favorable. Normally, sulfur, chlorine, and phosphorous containing organic compounds have been employed in the forming fluids for the Al alloy. The above mentioned organic molecules as lubricant additives play a significant role in the formation of a tribo-chemical

film on the contact surfaces to resist the local contact pressure. However, the poor stability of these additives during the process of applications does not meet the demands of new generation mechanical devices [11]. Additionally, the use of chlorine and phosphorus containing compounds is currently the focus of environmental concerns [12]. As a result, there is continuous research for the investigation of environmentally acceptable and efficient lubricant oil additives [13]. To date, many studies have shown that the lubrication performances for magnesium alloy/steel pairs could be significantly improved by introducing N-containing compounds [14], borates [15], and ionic liquids [16] into mineral oil. It was found that all of the compounds mentioned above as lubricant additives can interact with the surface of the magnesium alloy and generate a tribo-chemical film, thus enhancing the lubrication performance. Unfortunately, many nitrogen heterocyclic compounds showed good abrasion resistance and corrosion inhibition, but the friction reduction property was undesirable [17]. The borate without an active element, i.e. nitrogen, sulfur, and chlorine, is invalid for friction reducing and wear resistance for magnesium alloy/steel pairs. Additionally, the borates are inclined to hydrolyze, leading to the liberation of an oil-insoluble and abrasive boric acid because of the electron-deficient boron [18]. The widespread application of ionic liquids has been hindered by problems related to the thermo-oxidation, corrosion, and the cost associated with preparation [19]. Therefore, developing lubricant additives for magnesium alloys is imperative.

Recently, the prospect of lubricant additives has been expanded with the advent of nanomaterials [20]. There are many reasons to select nanoparticles as a lubricant additive. The essential feature is their nano-scale size that allows the particles to enter the contact area, and therefore the lubricant performance is improved. In addition, nanoparticles are being seen as one of the best possible options to save the environment from further pollution and degradation [21]. Different researchers have tried a variety of nanomaterial-dispersed base oil to enhance friction reduction and anti-wear behavior. Among these nano-based additives, it is reported that SiO<sub>2</sub> nanoparticles are considered as a hard and brittle material easily obtained on the market in a broad range of sizes at low cost, and have been studied for the machining and drilling of Al alloy [22,23]. These results showed that an oily nano-SiO<sub>2</sub> suspension was an effective lubricant providing low friction coefficient and excellent surface quality of the product. They proposed that the lubricating properties of the SiO<sub>2</sub> nanoparticles were a result of an efficient rolling mechanism at the tool-chip interface. Furthermore, MoS<sub>2</sub> nanoparticles are arguably the most common lubricant additive. The early studies reported that MoS<sub>2</sub> nanoparticles very effectively reduce the friction and wear in the boundary-lubrication for steel-steel pairs [24,25] and titanium-steel contacts [26], and can also enhance the lubrication even on relatively inactive surfaces, such as diamond-like carbon coating/steel contacts [27,28]. The key mechanism for reducing friction and wear is associated with the weak Vander Waals interaction between layers and the formation of a tribo-chemical film on the interface. In our previous work, the tribological performances of MoS<sub>2</sub> nanoparticles and SiO<sub>2</sub> nanoparticles as additives in oil-based lubricants were investigated by a ball-on-flat tribometer for magnesium alloy/steel pairs and we found that MoS<sub>2</sub> nanoparticles possess better anti-wear performance than SiO<sub>2</sub> nanoparticles, while SiO<sub>2</sub> nanoparticles obtain better dispersion in lubricating oil than MoS<sub>2</sub> nanoparticles [29]. Although individual MoS<sub>2</sub> nanoparticles or SiO<sub>2</sub> nanoparticles showed some enhanced tribological properties, the SiO<sub>2</sub>/MoS<sub>2</sub> hybrids as lubricant additive were expected to be more interesting.

The purpose of the present work is to determine the tribological effect of the combinative addition of MoS<sub>2</sub> nanoparticles and SiO<sub>2</sub> nanoparticles into the mineral oil to be used for magnesium alloy forming lubricants by a reciprocating mode of ball-on-flat [30]. The tribological performances of SiO<sub>2</sub>/MoS<sub>2</sub> hybrid nanolubricants were evaluated in comparison with the individual nano-MoS<sub>2</sub> at a concentration of 1.0 wt % in mineral oil. Furthermore, the lubrication mechanism is discussed in detail by examining the worn surfaces on the tested flats. This paper paves the way to further studies of magnesium alloys with nanolubrication.

## 2. Experimental

### 2.1. Materials

A common mineral oil (EOT5#) was selected as the base oil in the present tribo-evaluation, which was widely employed in the cold forming process of non-ferrous metal. The primary characteristics of the base oil are shown in Table 1. Based on the information provided by the supplier (Hasitai Lubricant Co., Ltd., Shanghai, China), we can exclude the existence of sulfur, phosphorus, and chlorine containing additives in the base oil.

The MoS<sub>2</sub> nanoparticles and SiO<sub>2</sub> nanoparticles used in this study were supplied by Nanjing Emperor Nano Material Co., Ltd. (Nanjing, China). The particle size and morphology of the nanoparticles were observed with Field Emission Scanning Electron Microscope (FESEM) and Transmission Electron Microscope (TEM) (Figure 1). The results showed that the MoS<sub>2</sub> nanoparticles have a flaky shape mostly with a length above 300 nm and a thickness of about 90 nm. The SiO<sub>2</sub> nanoparticles have a spherical shape with a diameter of 30 nm. The optimum nano-MoS<sub>2</sub> concentration (1.0 wt %) obtained by the previous screen test was adopted for the additives in the test [29]. The different concentrations of nano-SiO<sub>2</sub> (0.05 wt %, 0.1 wt %, 0.2 wt %, 0.5 wt %, 0.7 wt %, 1.0 wt %) mixed with 1.0 wt % nano-MoS<sub>2</sub> was added to EOT5# mineral oil by ultrasonication for 2 h to acquire a series of homogeneous nanolubricants. For comparison, 1.0 wt % MoS<sub>2</sub> nanolubricants and 0.1 wt % SiO<sub>2</sub> nanolubricants were prepared with the same procedure. Dispersants were not used in order to isolate the influence of the nanoparticles as lubricant additives.

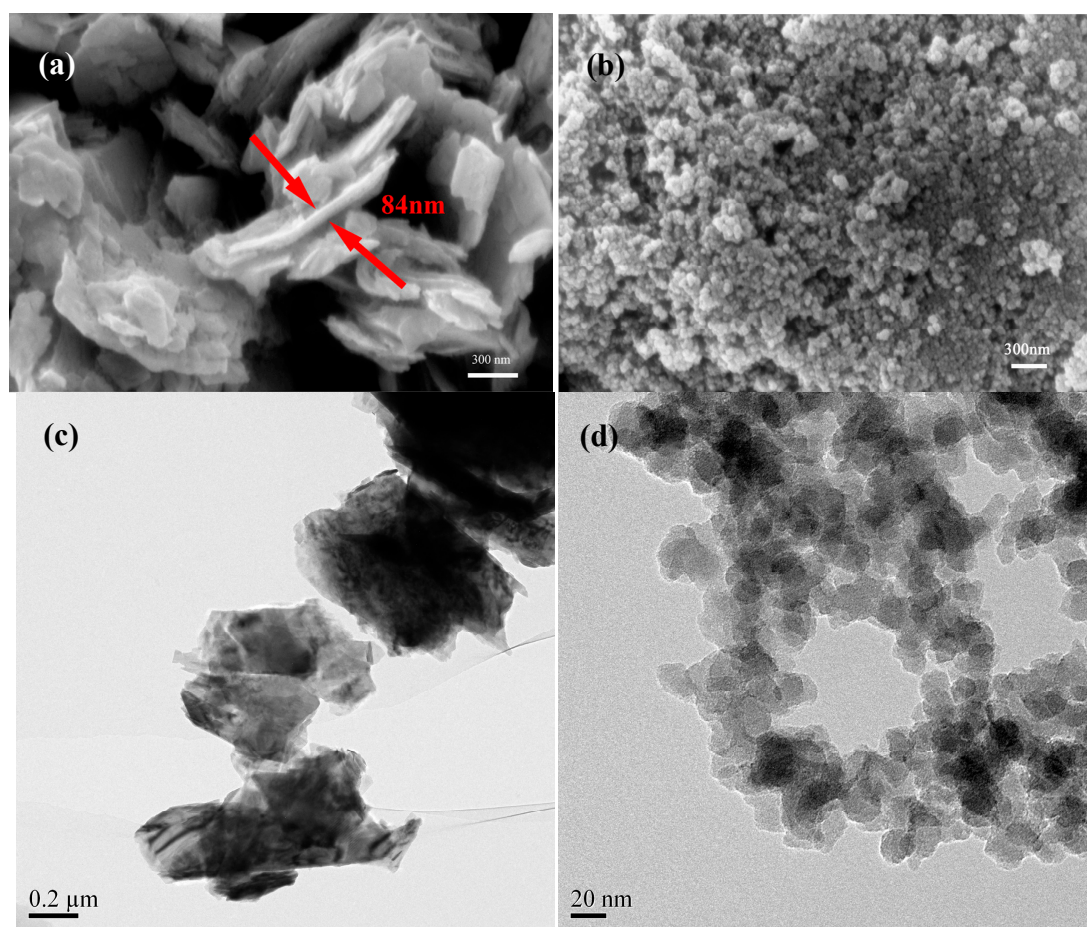
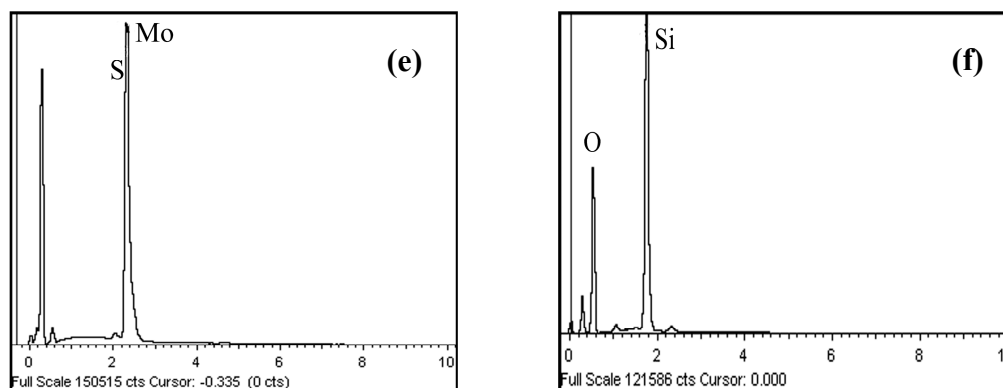


Figure 1. Cont.



**Figure 1.** FESEM micrograph, TEM image, and EDS spectra of MoS<sub>2</sub> nanoparticles (a,c,e) and SiO<sub>2</sub> nanoparticles (b,d,f).

**Table 1.** The primary characteristics of the EOT5# lubricant oil.

Primary Characteristics	Kinematic Viscosity (40 °C)	Density (15 °C)	Content of Saturates	Content of Aromatics	Contents of Sulfur
EOT5# lubricant oil	5.11 mm <sup>2</sup> /s	0.856 g/cm <sup>3</sup>	>90%	<1%	<0.03%

## 2.2. Friction and Wear Tests

The friction reducing and anti-wear properties of the base oil and the nano-material dispersed oils were evaluated by a reciprocating mode of the ball-on-flat tribometer (CSM Instruments, Peseux, Switzerland). The upper ball used in this study is AISI 52,100 bearing steel with a hardness of  $697 \pm 17$  kgf/mm<sup>2</sup>. The diameter of the ball is 6 mm and the average surface roughness of the ball is approximately 0.05  $\mu$ m. The lower specimens, 10 mm  $\times$  20 mm  $\times$  3 mm in size, made of an extruded AZ31 magnesium alloy sheet ( $R_a = 0.08$   $\mu$ m,  $H_v = 66.7$  kgf/mm<sup>2</sup>), were tested. Firstly, the effect of the SiO<sub>2</sub>/MoS<sub>2</sub> mixing ratio (wt/wt) on the lubrication properties of the nanolubricants was investigated. The applied load in this study was 3 N (312 MPa of maximum Hertzian contact stress), which is at least 30% higher than the yield strength of the AZ31 magnesium alloy sheets. The sliding speed was selected as 0.08 m/s, and the duration of the test was 30 min. The optimal proportion of the SiO<sub>2</sub>/MoS<sub>2</sub> hybrids was gained from the experiments mentioned above. Later, the effect of load on the mean friction coefficient was also studied by varying the loads (1, 3, 5, and 8 N) in a 30 min test. Finally, in order to evaluate the lubrication film stability, the normal load was increased to 8 N (446 MPa of the maximum Hertzian contact pressure), the sliding speed was decreased to 0.03 m/s, and the test time was extended to 1.5 h. All of the friction tests were conducted under ambient conditions. Prior to the frictional test, sufficient lubricant was dropped onto the ball-flat contact area. Three sets of tests at the same normal load and sliding speed were carried out to acquire each datum point to validate the repeatability and precision of the test results. Each experimental point indicates an average value of the experimental tests.

The lubrication conditions in tribological contacts contain the boundary lubrication, mixed lubrication, and hydrodynamic lubrication. The boundary lubrication is especially significant for metal forming operations. Therefore, in order to simulate the metal forming process by tribological tests, the corresponding lubrication conditions should be first determined in accordance with the  $\lambda$  ratio in Equation (1), where  $h_{\min}$  refers to the minimum film thickness separating the surfaces. The  $h_{\min}$  is evaluated by the Hamrock-Dowson model given in Equation (2), and  $R_q$  is the composite roughness determined by Equation (3),

$$\lambda = \frac{h_{\min}}{R_q} \quad (1)$$

$$h_{\min} = 2.8R' \left( \frac{\eta u_e}{E'R'} \right)^{0.65} \left( \frac{W_y}{E'R'^2} \right)^{-0.21} \quad (2)$$

$$R_q = \sqrt{R_{\text{ball}}^2 + R_{\text{flat}}^2} \quad (3)$$

where  $W_y$  is the applied load (3 N),  $R$  is the radius of the ball (6 mm),  $u_e$  is the speed (0.08 m/s),  $\eta$  is the dynamic viscosity of the nanolubricants, and  $E'$  and  $R'$  are the elastic modulus and effective radius for the sliding surface, respectively. The lubrication regime is generally considered by the following regulations:  $0.1 < \lambda < 1$  indicates boundary lubrication;  $1 \leq \lambda \leq 3$  indicates mixed lubrication, and  $\lambda > 3$  indicates elastohydrodynamic lubrication [31]. Using the corresponding values of the fundamental constants of physics and material characteristics, the thickness of the lubricant film at the point of contact is 35 nm for 3 N at 0.08 m/s and a lambda ratio of 0.37, and therefore within the boundary lubrication regime.

### 2.3. Worn Surface Analysis

After testing, the magnesium alloy flats were ultrasonically cleaned in acetone and dried in air. The wear volume on the tested flats was measured by an Olympus OLS40003D surface microscope profiler, and each scar was measured at least three times under the same conditions. The morphologies and element compositions of the worn surfaces were characterized by a Zeiss AURIGA FESEM (Zeiss; Oberkochen, Germany) equipped with an EDAX GENESIS EDS. The acceleration voltage was set at 10 kV and the working distance at 10 mm. Furthermore, the chemical species on the worn surfaces were evaluated by X-ray Photoelectron Spectroscopy (XPS, VG model Escalab 250, VG Scientific Ltd., East Grinstead, UK). The X-rays were monochromatic Al-K $\alpha$  photons, and the binding energy was corrected by the adventitious C1s peak at 284.6 eV. The XPS spectra were obtained with an analyser pass energy of 29 eV, and the precision of the binding energy tests is about 0.6 eV. The measured area was approximately 500  $\mu\text{m}$  in diameter. The acquired peaks were then fitted with Gaussian–Lorentzian curves after subtraction of a Shirley background using CASA XPS software (Casa software Ltd., East Grinstead, UK).

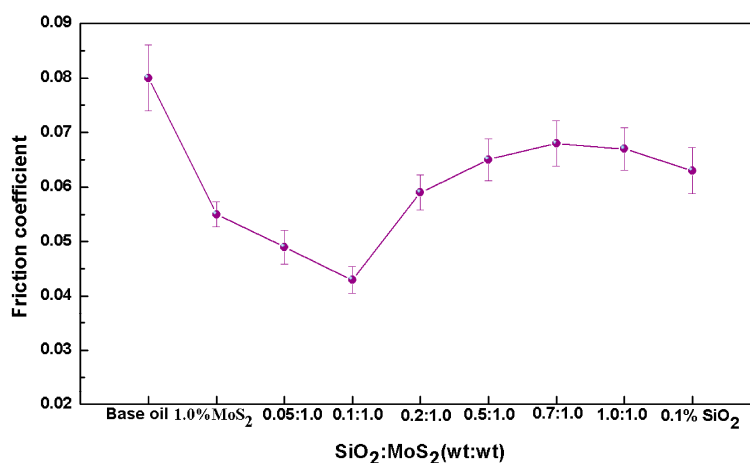
## 3. Results and Discussion

### 3.1. Friction and Wear Performances

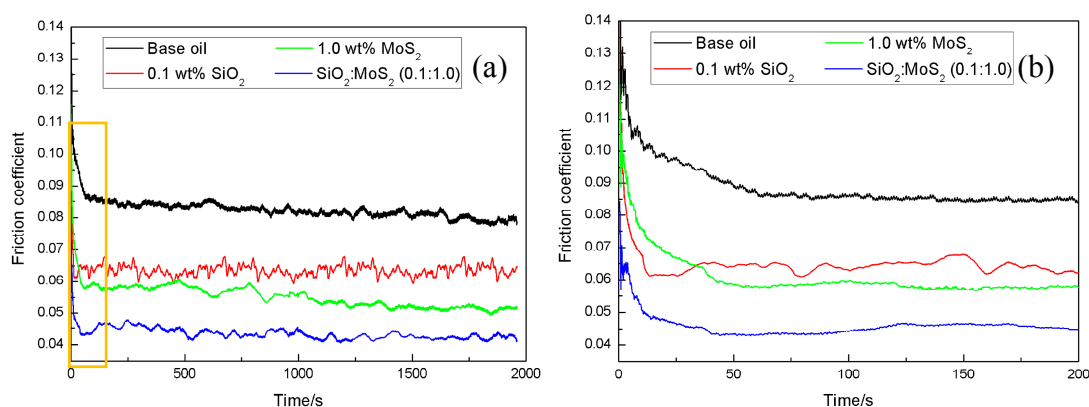
To investigate the tribological properties of the SiO<sub>2</sub>/MoS<sub>2</sub> hybrid nanolubricants, different mixing ratios of SiO<sub>2</sub>/MoS<sub>2</sub> hybrid nanolubricants were prepared to test the best working conditions. Figure 2 displays the average friction coefficient of the magnesium alloy-steel pairs lubricated by various SiO<sub>2</sub>/MoS<sub>2</sub> hybrid nanolubricants as compared with those of the individual nanolubricants at a normal load of 3 N, a sliding speed of 0.08 m/s, and the duration of 0.5 h. These nanomaterial dispersed oils show smaller friction coefficients than the base oil. This result suggests that all these nanomaterials as lubricant additives have positive effects on enhancing the friction reducing performance of the base oil. Even so, the friction-reducing efficiencies of these samples are disparate. It is observed that the friction coefficient gradually decreases with the increase of the concentration of the SiO<sub>2</sub> nanoparticles in the SiO<sub>2</sub>/MoS<sub>2</sub> hybrid nanolubricants, while a higher concentration of nano-SiO<sub>2</sub> will deteriorate the friction reducing performance, which is even worse than those of the nano-MoS<sub>2</sub> alone. Consequently, when the quantity of nano-SiO<sub>2</sub> in the SiO<sub>2</sub>/MoS<sub>2</sub> hybrid nanolubricants reaches an optimal concentration, a significant friction-reduction effect is obtained. For instance, when 0.1 wt % of nano-SiO<sub>2</sub> is added in the SiO<sub>2</sub>/MoS<sub>2</sub> hybrid nanolubricants, the minimum friction is acquired. The optimal concentration of nano-SiO<sub>2</sub> in the SiO<sub>2</sub>/MoS<sub>2</sub> nanolubricants reduced the friction coefficient by 21.8% compared with the 1.0 wt % MoS<sub>2</sub> nanolubricants.

Figure 3 illustrates the initial part of the friction coefficient curve for magnesium alloy/steel contacts supplemented with base oil and nanolubricants. From Figure 3, it can be seen that the friction-reducing behavior of the 1.0 wt % MoS<sub>2</sub> nanolubricants is slightly inferior to that of the 0.1 wt %

SiO<sub>2</sub> nanolubricants at the initial stage of the tests. Comparable evolution of the friction coefficient with time for steel-steel pairs lubricated by 1.0 wt % MoS<sub>2</sub> nanolubricants, where a higher coefficient of friction at the initial stage of the tests can be observed, were described by L. Cizaire et al. [32]. These references indicate that the coefficient of friction is higher at the start of the tests due to the absence of the tribo-chemical film. Nonetheless, once the tribo-chemical film is generated on the contact surface during the sliding process, the friction coefficient decreased rapidly. This suggests that the tribo-chemical film provides a vital role in the friction reducing properties. The results were also verified by other studies [33]. Unlike MoS<sub>2</sub> nanoparticles, SiO<sub>2</sub> nanoparticles possess nano-scale size and excellent dispersion in the base oil. These properties allow the SiO<sub>2</sub> nanoparticles to easily move into the contact area, thus resulting in faster running-in conditions. This is regarded as the primary reason why the friction-reducing property of 0.1 wt % SiO<sub>2</sub> nanolubricants is more pronounced than that of 1.0 wt % MoS<sub>2</sub> nanolubricants at the beginning stage of the tests. In sharp contrast, the friction coefficient of the SiO<sub>2</sub>:MoS<sub>2</sub> (0.1:1.0) hybrid nanolubricants quickly decreases and stabilizes at a lower value than that of the 1.0 wt % MoS<sub>2</sub> nanolubricants or 0.1 wt % SiO<sub>2</sub> nanolubricants. This suggests that the synergistic effect of SiO<sub>2</sub> and MoS<sub>2</sub> during sliding can effectively reduce the time of the running-in stage.



**Figure 2.** The average friction coefficient as a function of different SiO<sub>2</sub>/MoS<sub>2</sub> nanolubricants for magnesium alloy-steel contacts (3 N, 0.08 m/s, 0.5 h).



**Figure 3.** (a) Variation in the friction coefficient as a function of time and (b) the initial part of the friction coefficient curve (amplification of the yellow box) for the base oil, 1.0 wt % MoS<sub>2</sub> nanolubricants, 0.1 wt % SiO<sub>2</sub> nanolubricants, and SiO<sub>2</sub>:MoS<sub>2</sub> (0.1:1.0) hybrid nanolubricants (3 N, 0.08 m/s, 0.5 h).

For the anti-wear performance, since the AISI 52100 steel ball in this study is harder than the AZ31 magnesium alloy flat, most of the wear tracks are not obvious and deep enough to accurately calculate the wear volume of the ball. Therefore, comparisons of the average wear volume and the 2D cross-section profiles of the worn surface on the corresponding AZ31 magnesium alloy lubricated by different samples are shown in Figure 4. As shown in Figure 4a, it was found that the anti-wear performance of the  $\text{SiO}_2/\text{MoS}_2$  hybrid additive is better than that of the single nano- $\text{SiO}_2$  or nano- $\text{MoS}_2$ . When an optimized concentration of nano- $\text{SiO}_2$  in the  $\text{SiO}_2/\text{MoS}_2$  hybrid nanolubricants reaches 0.1 wt %, the decrease of the wear volume is about 8.6% as compared with the 1.0 wt %  $\text{MoS}_2$  nanolubricants. Similar to the friction reducing effect, further increasing the concentration of the nano- $\text{SiO}_2$  will deteriorate the anti-wear performance. As can be observed from the 2D cross-section profiles of the wear tracks lubricated by different lubrications in Figure 4b, the  $\text{SiO}_2:\text{MoS}_2$  (0.1:1.0) hybrid additive exhibited shallower wear tracks than individual  $\text{SiO}_2$  or  $\text{MoS}_2$  did. In this case, the appropriate mass ratio of nano- $\text{SiO}_2$  and nano- $\text{MoS}_2$  appeared at 0.1:1.0. Therefore,  $\text{SiO}_2:\text{MoS}_2$  (0.1:1.0) hybrid nanolubricants were selected for further study.

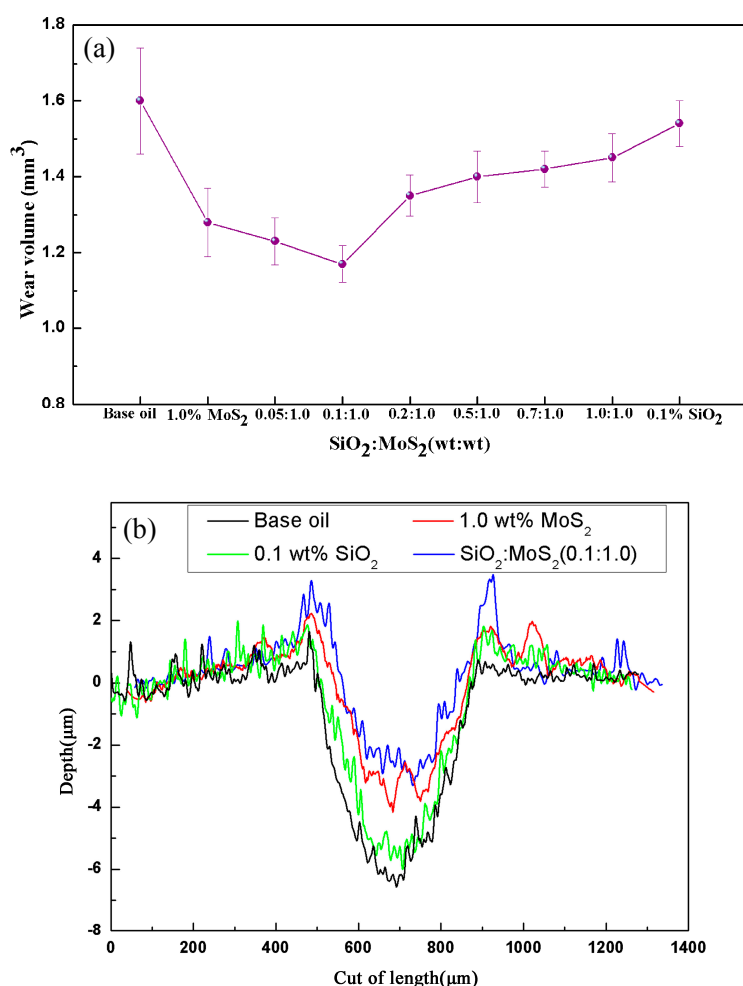


**Figure 4.** (a) Wear volume and (b) 2D cross-section profiles of the worn surface on the magnesium alloy as a function of different nanolubricants (3 N, 0.08 m/s, 0.5 h).

### 3.2. The Capacity of Carrying Load

Figure 5 depicts the average friction coefficient as a function of the load for the base oil, 0.1 wt %  $\text{SiO}_2$  nanolubricants, 1.0 wt %  $\text{MoS}_2$  nanolubricants, and  $\text{SiO}_2:\text{MoS}_2$  (0.1:1.0) hybrid nanolubricants (speed, 0.08 m/s, time, 30 min.). It is observed that the friction coefficient increases with the increase

of normal load for the base oil and 0.1 wt %  $\text{SiO}_2$  nanolubricants. This is most probably because the micro-intervals between the friction pairs decrease with an increase of the normal load. Therefore, there is less base oil that could enter into the frictional interface, resulting in an increase in the direct contact of the surface asperities. In the case of the 0.1 wt %  $\text{SiO}_2$  nanolubricants, spherical  $\text{SiO}_2$  nanoparticles may act as nano-bearings between the moving parts, thus improving the friction reduction properties. However, we need to mention that the roller bearing effect of the spherical nanoparticles during sliding is very deeply inclined with the operating conditions. The references [34,35] reported that the shape of the nanoparticles is obscured if the lubricant film thickness between the two surfaces gets close to the size of the spherical nanoparticles. In this study, the minimum film thickness ( $h_{\min}$ ) calculated according to the Hamrock-Dowson equation is 44 nm, 35 nm, 31 nm, and 28 nm for 1 N, 3 N, 5 N, and 8 N, respectively. It is indicated that the lubricant film thickness between the contact surfaces decreases with increasing load, which is getting close to the size of the spherical  $\text{SiO}_2$  nanoparticles. Consequently, the shape of the nanoparticles is obscured during rubbing, resulting in an increase in the friction coefficient. That may be why the friction coefficient for 0.1 wt %  $\text{SiO}_2$  nanolubricants increased with increasing the applied load, although it still remains lower than that of the base oil. The friction behaviors of the 1.0 wt %  $\text{MoS}_2$  nanolubricants and the  $\text{SiO}_2\text{:MoS}_2$  (0.1:1.0) hybrid nanolubricants are found to be quite different from the base oil and the 0.1 wt %  $\text{SiO}_2$  nanolubricants at the same experimental conditions. The friction coefficient for the 1.0 wt %  $\text{MoS}_2$  nanolubricants and  $\text{SiO}_2\text{:MoS}_2$  (0.1:1.0) hybrid nanolubricants decreases gradually with increasing load. These results reflect the fact that the friction-reducing property of the 1.0 wt %  $\text{MoS}_2$  nanolubricants or  $\text{SiO}_2\text{:MoS}_2$  (0.1:1.0) hybrid nanolubricants gradually strengthens with increasing load. With the increasing load, the  $\text{MoS}_2$  nanoparticles easily interact with the new-exposed contact surfaces. This is conducive to the formation of the tribo-chemical film on the surface, thereby decreasing the friction coefficient. Additionally, from an atomistic and computational aspect [36–38], the repulsive contribution of the Lennard-Jones potential increases with an increase in the applied load, thus offering the “ground” for better sliding and a lower friction coefficient.

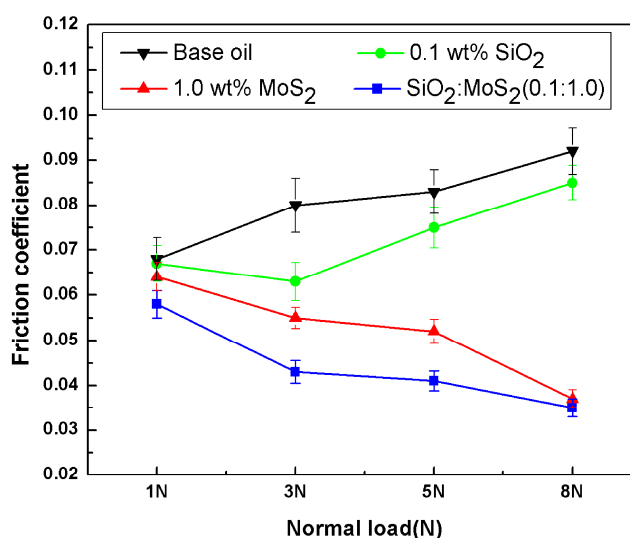


**Figure 5.** Friction coefficients for the base oil and nanolubricants under four different loads (0.08 m/s, 0.5 h).

### 3.3. Lubrication-Film Stability

In order to investigate the stability of the lubrication-film during rubbing in more extreme test conditions, the tribological experiments were conducted at a load of 8 N and sliding speed of 0.03 m/s for 1.5 h. Variations of friction coefficients of the base oil, 0.1 wt %  $\text{SiO}_2$  nanolubricants, 1.0 wt %  $\text{MoS}_2$  nanolubricants, and the  $\text{SiO}_2\text{:MoS}_2$  (0.1:1.0) hybrid nanolubricants with increasing sliding time are

shown in Figure 6. As shown in Figure 6a, a general order of friction coefficient values is observed as follows:  $\text{SiO}_2\text{:MoS}_2$  (0.1:1.0) hybrid nanolubricants < 1.0 wt %  $\text{MoS}_2$  nanolubricants < 0.1 wt %  $\text{SiO}_2$  nanolubricants < base oil. The friction coefficient for the base oil presented acute fluctuations after about 230 s of sliding. The high friction coefficient with dramatic fluctuations is a classic indication of lubrication failure resulting in the contact surface scuffing and the propagation of scuffing damage [39]. When 0.1 wt %  $\text{SiO}_2$  nanoparticles were dispersed into the base oil, the friction coefficient had little difference to the base oil at the early stage of the test, as they were all about 0.11. As the test duration increased, the friction coefficient became lower and less noisy. During the sliding, nano- $\text{SiO}_2$  was possibly adsorbed onto the contact areas to present the rolling effect like miniature bearings, and thus the friction coefficient decreased gradually [40]. The third curve is the 1.0 wt %  $\text{MoS}_2$  nanolubricants. The presence of nano- $\text{MoS}_2$  reduced the friction coefficient from 0.11 to about 0.077 in the first 20 min, after which the friction coefficient approached a steady state and lasted for the entire tribological test. Interestingly, the friction-reducing behavior of 1.0 wt %  $\text{MoS}_2$  nanolubricants or 0.1 wt %  $\text{SiO}_2$  nanolubricants has little difference at the early stage of the tests (Figure 6b). Compared with the tribological tests in Figure 3, it is more difficult for  $\text{MoS}_2$  or  $\text{SiO}_2$  nanoparticles to enter the contact area at the early stage due to the higher load in the lubrication-film stability tests. Therefore, it can be inferred that the nanoparticle additives in the base lubricant have little impact on the friction coefficient at the initial stage of the tests. In contrast, the friction coefficient of the  $\text{SiO}_2\text{:MoS}_2$  (0.1:1.0) hybrid nanolubricants was quite different from the other samples. The beginning stage of the friction coefficient dramatically reduced, and gradually stabilized in the latter part of the curve. The results illustrated that the  $\text{SiO}_2$  nanoparticles can achieve a synergic function on the friction reducing abilities of nano- $\text{MoS}_2$  even under harsh tribo-conditions.

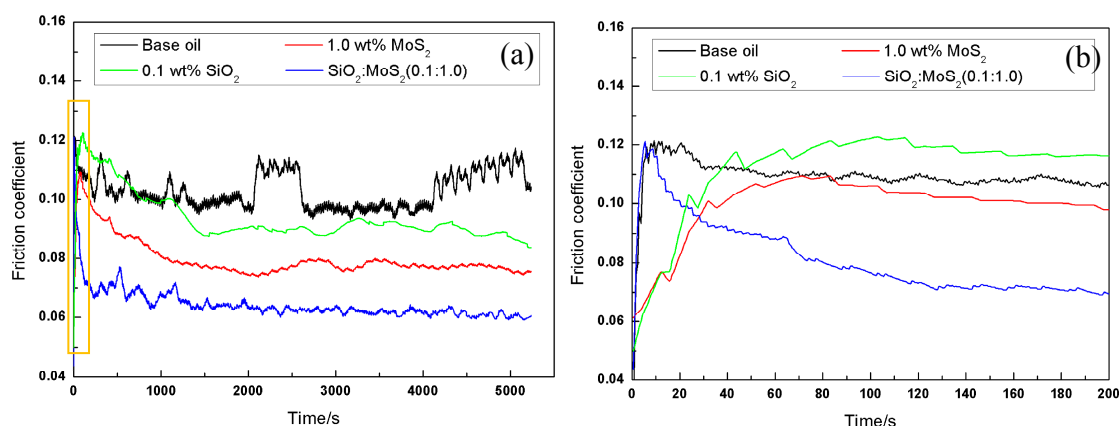


**Figure 6.** (a) Sliding time to lubrication-film break down and (b) the initial part of the friction coefficient curve (amplification of the yellow box) for the base oil, 1.0 wt %  $\text{MoS}_2$  nanolubricants, 0.1 wt %  $\text{SiO}_2$  nanolubricants, and  $\text{SiO}_2\text{:MoS}_2$  (0.1:1.0) hybrid nanolubricants (8 N, 0.03 m/s, 1.5 h).

### 3.4. FESEM and XPS Analyses of the Worn Surfaces

To further evaluate the effect of different lubricants on the tribological mechanism, Figure 7 shows the FESEM images of the worn surface on the AZ31 magnesium alloy after sliding for 30 min at 3 N and 0.08 m/s. As expected, the wear scar lubricated by the base oil is very rough. Numerous ridges and grooves on the entire wear scar can be found, which indicates that the base oil is not efficient at protecting the rubbing surface. For the 0.1 wt %  $\text{SiO}_2$  nanolubricants, the worn surface shows apparent scuffing accompanied with wear debris. The hard nano- $\text{SiO}_2$  plows the soft magnesium alloy surfaces under the applied load, which resulted in the abrasive wear. Even so, the severe scuffing damages for the  $\text{SiO}_2$  nanolubricants are greatly reduced when compared to the base oil. It is indicated that  $\text{SiO}_2$  nanoparticles as a lubricant additive improves the anti-wear behavior of the base oil, while when the base oil is formulated with 1.0 wt % nano- $\text{MoS}_2$ , the wear process further slows down. The furrows on

this wear surface become flat and smooth and the furrow numbers are also decreased. Some scattered black remnants are observed in Figure 7c, indicating that a tribo-chemical film may be generated during the rubbing process. The transfer film improved the anti-wear properties by protecting the direct contact between the magnesium alloy-steel pairs. In marked contrast, the  $\text{SiO}_2\text{:MoS}_2$  (0.1:1.0) hybrid nanolubricants produce even less surface damage with the smoothest worn surface and fewest grooves in a more random pattern. More importantly, a more compact tribofilm is formed on the worn surface (Figure 7d). It again proves that  $\text{SiO}_2/\text{MoS}_2$  hybrids as lubricant additives can dramatically reduce the friction and wear for magnesium alloys/steel contacts. The FESEM images of the worn surface are consistent with the measured tribological characteristics.

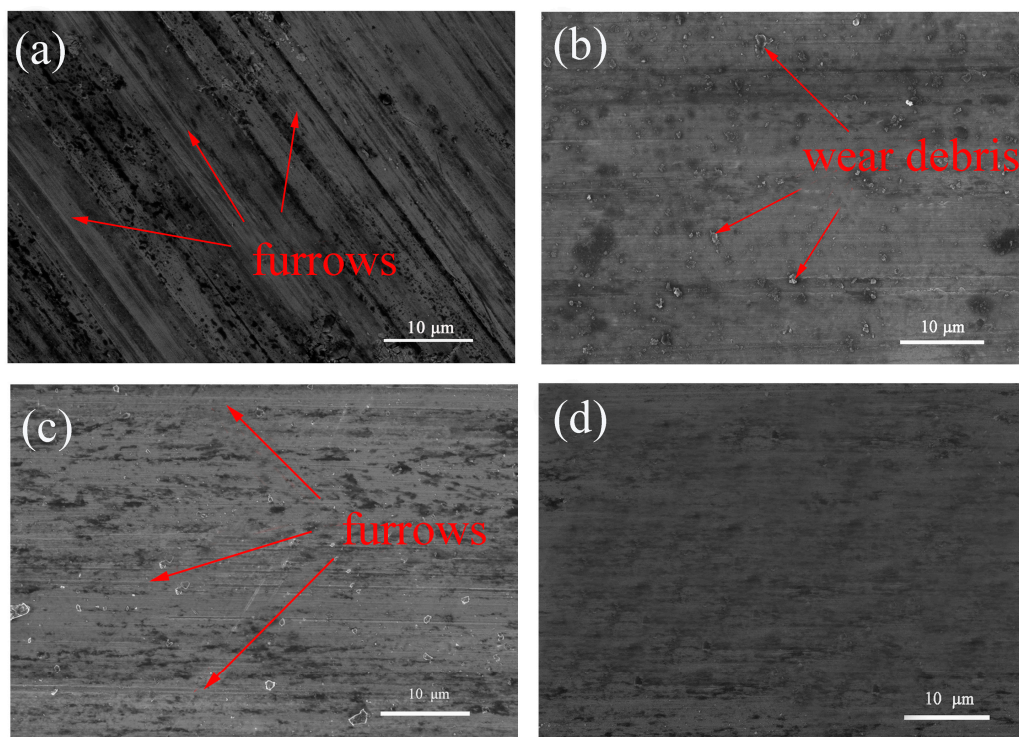


**Figure 7.** FESEM images of the worn surfaces on the magnesium alloy lubricated by: (a) base oil, (b) 0.1 wt %  $\text{SiO}_2$  nanolubricants, (c) 1.0 wt %  $\text{MoS}_2$  nanolubricants, and (d)  $\text{SiO}_2\text{:MoS}_2$  (0.1:1.0) hybrid nanolubricants (3 N, 0.08 m/s, 0.5 h).

To investigate the chemical composition of the tribofilm, the XPS spectra of the worn surface on the magnesium alloy lubricated by  $\text{SiO}_2\text{:MoS}_2$  (0.1:1.0) hybrid nanolubricants has been recorded. As shown in Figure 8, the spectrum of  $\text{Mg}2p$  (Figure 8a) shows a peak at the binding energy of 49.5 eV, which was attributed to the chemical state of the metallic magnesium. The  $\text{Mo}3d$  (Figure 8b) peaks appeared at 228.3 eV and 231.5 eV. The former combined with the  $\text{S}2p$  peaks at 161.2 eV is assigned to  $\text{MoS}_2$  [41]. The latter combined with the  $\text{O}1s$  peak at 530.2 eV is assigned to  $\text{MoO}_3$  [42]. The  $\text{MoS}_2$  signal indicates that nano- $\text{MoS}_2$  has been deposited on the contact surfaces and forms a physical protecting film on the flat. Furthermore, the  $\text{MoO}_3$  signal suggests that a few  $\text{MoS}_2$  nanoparticles deposited on the contact surfaces have been oxidized during the rubbing process. The  $\text{S}2p$  peak appears at approximately 169.4 eV, combined with the binding energy of  $\text{O}1s$  532.4 eV, indicating the generation of  $\text{MgSO}_4$  [20]. The amount of  $\text{MgSO}_4$  is not enough to affect the XPS spectrum of the main element Mg in Figure 8a. The  $\text{MgSO}_4$  signal also indicates that nano- $\text{MoS}_2$  has reacted with the magnesium alloy surface during the sliding process, and thus a new chemical transfer film formed on the worn surface. Furthermore, the  $\text{Si}2p$  spectrum (Figure 8d), associated with the  $\text{O}1s$  peak at 531.6 eV, shows a dominant peak at 103.2 eV assigned to  $\text{SiO}_2$  [43]. It is deduced that the  $\text{SiO}_2$  nanoparticles

cooperated with the MoS<sub>2</sub> nanoparticles to lubricate the surface of the magnesium alloy. Therefore, it can be reasonably concluded that the SiO<sub>2</sub>/MoS<sub>2</sub> hybrid nanolubricants have proven their remarkable friction reducing and anti-wear behaviors through generating a complicated boundary lubrication film that mainly consists of MoO<sub>3</sub> and MgSO<sub>4</sub> via chemical reaction plus the absorbed nanomaterial which comes from the lubricant additive itself.

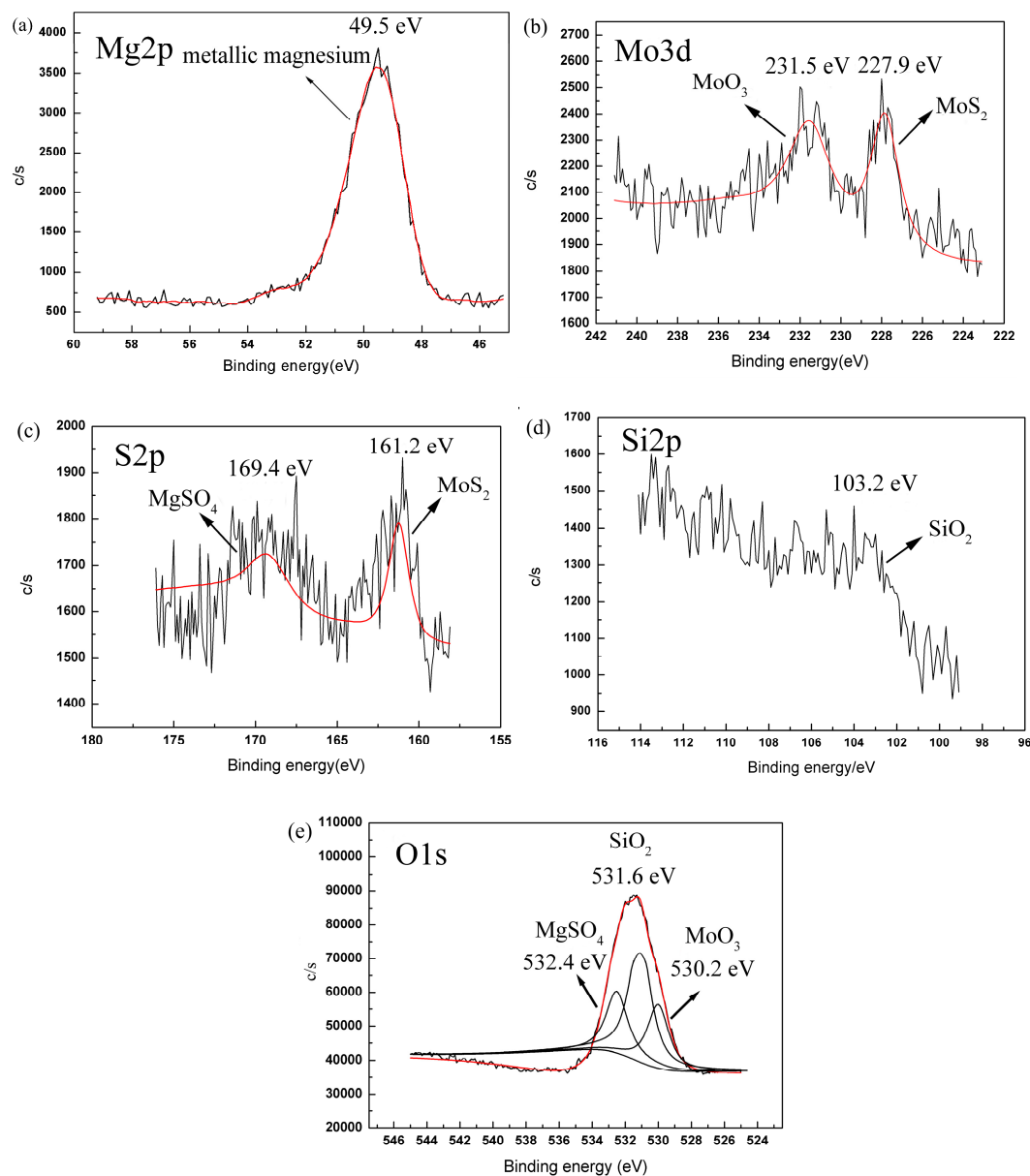


**Figure 8.** XPS spectra of (a) Mg2p, (b) Mo3d, (c) S2p, (d) Si2p, (e) O1s on the wear scars lubricated with SiO<sub>2</sub>:MoS<sub>2</sub> (0.1:1.0) hybrid nanolubricants. (3 N, 0.08 m/s, 0.5 h).

### 3.5. Lubrication Mechanism of SiO<sub>2</sub>/MoS<sub>2</sub> Hybrid Nanolubricants

The above tribological results suggest that both friction reduction and wear resistance behaviors can be dramatically improved for the combinative addition of MoS<sub>2</sub> nanoparticles and SiO<sub>2</sub> nanoparticles into the base oil. In order to deeply understand the lubricant mechanism that is underlying the trends observed in the lubrication responses, the high magnification FESEM-EDS spectra of the worn surfaces lubricated by the SiO<sub>2</sub>:MoS<sub>2</sub> (0.1:1.0) hybrid nanolubricants and SiO<sub>2</sub>:MoS<sub>2</sub> (0.5:1.0) hybrid nanolubricants are chosen for detailed analyses in Figure 9. As shown in Figure 9a, it is

clearly seen that the large particles deposit on the flat of the worn surfaces, while the granular particles fill up the grooves of the rubbing surfaces. Based on the EDS results, the large particles (point 1) are validated as  $\text{MoS}_2$ , and the granular particles (point 2) are considered to be  $\text{SiO}_2$ . It is suggested that the distribution of nanoparticles on the worn surface is substantially different on the microcosmic scale. The composition of the point 3 includes Mg, Al, O, S, and C. Combined with the XPS results, it is identified as  $\text{MgSO}_4$ . As mentioned above, the nano- $\text{MoS}_2$  protects the surface of the magnesium alloy in two ways. First of all, the  $\text{MoS}_2$  nanoparticles could be assembled on the rubbing surface due to the traction and compression formed by high contact stress. Intrinsically, the  $\text{MoS}_2$  shares the common structure of stiff, strongly bound planes held together by weak interlayer forces, which is what favors their sliding capability. The particular structure can provide low resistance for shear which thus results in friction reduction and wear resistance enhancement. Secondly, under the conditions of high pressure and high flash temperature caused by friction, the diffused  $\text{MoS}_2$  nanoparticles on the surface took tribo-chemical reaction with the rubbing surface to form molybdenum oxidized and magnesium sulfate, which had been demonstrated in the XPS analysis. The reaction mechanism can be directly compared with those acquired in the literature concerning the interactions of the  $\text{MoS}_2$  nanoparticles with the steel surface [41]. The reference described the possibilities as follows. One possibility is that the tribo-chemical film adhesion through the bonding of molybdenum with the oxygen was found in the oxide layer of the native steel surface. Therefore, a chemical reaction between molybdenum and the oxygen from  $\text{MgO}$  is chemically reasonable. The fact that the chemical reaction occurs between  $\text{MgO}$  and the  $\text{MoS}_2$  nanoparticles could be understood by a lower energy bonding between Mg and O than between Fe and O according to the Pearson hardness. Another possibility is that the oxide layer is quasi-immediate, wearing off at the early stage of the test, followed by S-Mg interactions and oxidization of the tribo-chemical film after its formation. The oxygen atoms could come from the air. Additionally, as in the past, it was proposed that water in the humid environment may prompt formation of  $\text{MoO}_3$  by direct oxidation. Giacomo Levita et al. [44] investigated the possibility of displacing a sulfur atom on the edge with the oxygen atom from the water molecule by ab initio calculations. The results showed that the  $\text{MoS}_2$  is more likely to absorb water along its edges instead of being oxidized by it at room temperatures. Even so, few experimental data have provided the evidence. To date, a complete understanding of the formation mechanism of the tribo-chemical film on the worn surface is still elusive. According to these results mentioned above, the adsorption of  $\text{MoS}_2$  nanoparticles, in conjunction with its reaction products with the magnesium alloy, forms a tribo-chemical film that dramatically improves the tribological behaviors.

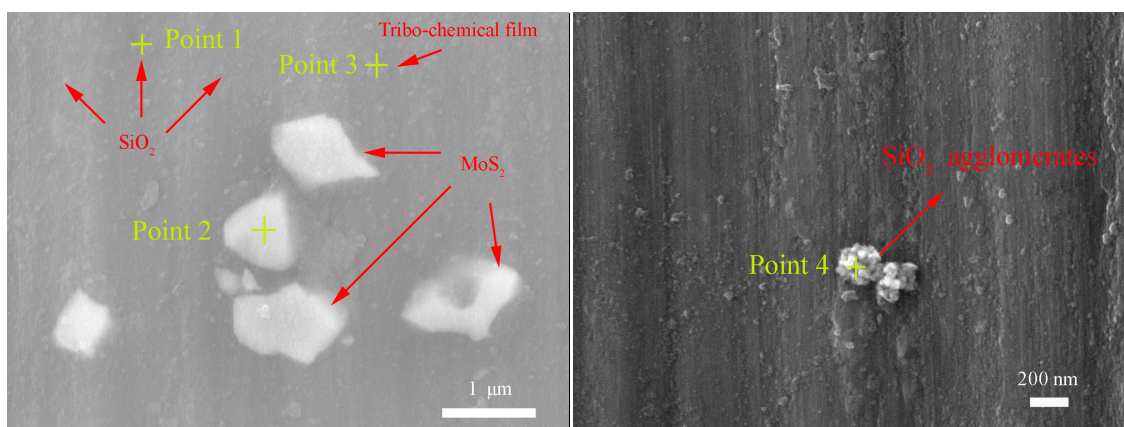
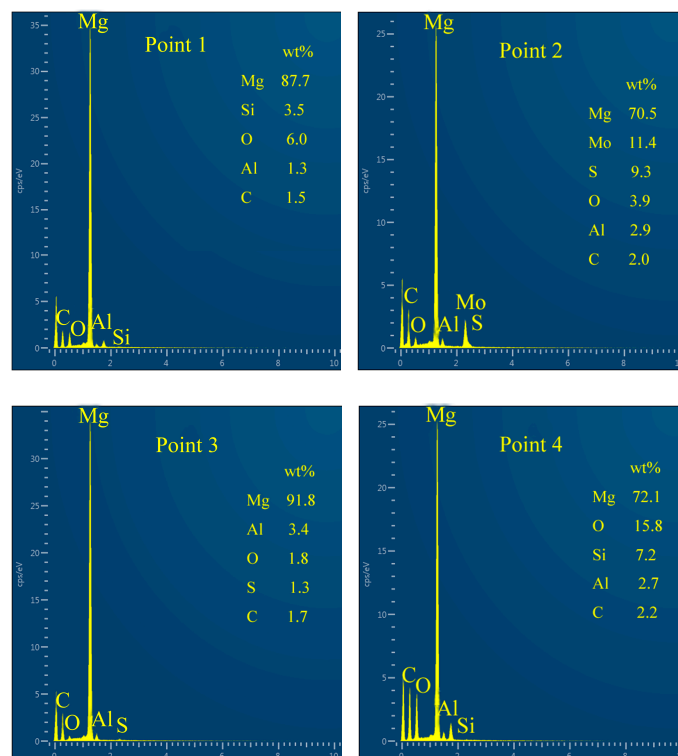


Figure 9. Cont.



**Figure 9.** High-magnification FESEM-EDS spectra of the worn surfaces of the magnesium alloy lubricated by the SiO<sub>2</sub>:MoS<sub>2</sub> (0.1:1.0) hybrid nanolubricants (a) and SiO<sub>2</sub>:MoS<sub>2</sub> (0.5:1.0) hybrid nanolubricants (b) (3 N, 0.08 m/s, 30 min).

In contrast, the friction reducing and anti-wear mechanism of spherical SiO<sub>2</sub> nanoparticles is distinctly different from that of the lamellar MoS<sub>2</sub> nanoparticles. Unlike nano-MoS<sub>2</sub>, nano-SiO<sub>2</sub> is more likely to enter the contact area due to its infinitesimally tiny size and outstanding dispersion in the base oil, thereby resulting in faster running in stage (Figure 3). The existence of the spherical nano-SiO<sub>2</sub> between the contact surfaces is often thought of as a wheel to help the easy sliding under normal load, although the rolling effect of nanoparticles as a lubricant additive is difficult to be directly observed during rubbing [45]. In this case, nanoparticles reduce the shear stress, thus resulting in friction reduction. Additionally, as reported by Mosleh Mohsen et al. [26], the filling of valleys of the contacting asperities will occur if the characteristic length  $l$  of flake-like nanoparticles is smaller than the peak-to-valley roughness of the harder surface which is equal to  $4Ra$ , i.e., the condition of  $l < 4Ra$  applies. For the spherical particles, the diameter  $d$  of the particle should satisfy  $d < 0.67Ra$ . Therefore, the second mechanism of the significantly improved tribological performance of spherical SiO<sub>2</sub> nanoparticles that are about 30 nm in diameter is ascribed to the fact that the nano-SiO<sub>2</sub> spheres act as a third body material filling in the original pits and valleys on the surface of the magnesium alloy flat with 0.08  $\mu\text{m}$  surface roughness, thus forming a thin physical film. The generated physical film is endowed with many crucial functions, including separating the contact surfaces to avert direct contact, enhancing the load-carrying capacity and decreasing the stress concentration. However, using nano-MoS<sub>2</sub> platelets may be hard to fill in the microgaps because their length is larger than  $4Ra$  in the present study. Micro-cooperation occurred in succession between the shearing-sliding of the lamellar MoS<sub>2</sub> nanoparticles and the filling of the spherical SiO<sub>2</sub> nanoparticles during the sliding process. This observation is supported by relevant FESEM-EDS analysis in the present research (Figure 9a). If super abundant SiO<sub>2</sub> nanoparticles were dispersed into the SiO<sub>2</sub>/MoS<sub>2</sub> hybrid nanolubricants, SiO<sub>2</sub> nanoparticles would tend to form irreversible agglomerates as shown in Figure 9b. The agglomerates limited the motion of nearby nanoparticles which generated a larger amount of stress concentrations

leading to worse lubricating efficacy [46]. Additionally, the SiO<sub>2</sub> nanoparticles possess excellent mechanical properties particularly with respect to the hardness ( $H_v = 1000 \text{ kgf/mm}^2$ ); consequently, the excess hard SiO<sub>2</sub> nanoparticles as an abrasive ploughs the soft surfaces of the magnesium alloy ( $H_v = 66.7 \text{ kgf/mm}^2$ ) under the normal load. It will accelerate the abrasion of the magnesium alloy surface during the sliding process, thereby leading to the worse wear resistance. This was also verified by the inferior tribological properties of the nanolubricants with a high content of SiO<sub>2</sub> nanoparticles, such as SiO<sub>2</sub>:MoS<sub>2</sub> (0.2:1.0), SiO<sub>2</sub>:MoS<sub>2</sub> (0.5:1.0), SiO<sub>2</sub>:MoS<sub>2</sub> (0.7:1.0), and SiO<sub>2</sub>:MoS<sub>2</sub> (1.0:1.0) in Figures 2 and 4. Therefore, SiO<sub>2</sub>:MoS<sub>2</sub> (0.1:1.0) hybrid nanolubricants exhibit the best tribological properties for synergetic lubrication even in the capacity of the carrying load and lubrication film stability tests. In view of the above-mentioned experimental results, a lubrication system based on the blends of SiO<sub>2</sub> nanoparticles and MoS<sub>2</sub> nanoparticles is established. The significant increase in the tribological performances by the SiO<sub>2</sub>/MoS<sub>2</sub> hybrids as lubricant additives enables the sustainable and energy conserving lubricant system.

#### 4. Conclusions

The tribological performances of nano-MoS<sub>2</sub>, nano-SiO<sub>2</sub>, and their hybrids as lubricant additives for magnesium alloy–steel pairs were evaluated using a reciprocating ball-on-flat tribotester. The conclusions can be summarized as follows from the experimental results.

- (1) 1.0 wt % MoS<sub>2</sub> nanolubricants, 0.1 wt % SiO<sub>2</sub> nanolubricants, and SiO<sub>2</sub>/MoS<sub>2</sub> hybrid nanolubricants presented superior friction-reducing and anti-wear behaviors as well as a high load-carrying capacity. The optimal friction reducing and anti-wear capability was obtained for the combinative addition of 1.0 wt % nano-MoS<sub>2</sub> and 0.1 wt % nano-SiO<sub>2</sub> into the base oil.
- (2) 0.1 wt % SiO<sub>2</sub> mixed with 1.0 wt % nano-MoS<sub>2</sub> addition into the base oil showed a 21.8% reduction in the friction coefficient and 8.6% reduction in the wear volume compared with the 1.0 wt % MoS<sub>2</sub> nanolubricants.
- (3) Under the lubrication of the SiO<sub>2</sub>:MoS<sub>2</sub> (0.1:1.0) hybrid nanolubricants, a complex tribo-chemical film that mainly contains MoO<sub>3</sub> and MgSO<sub>4</sub> through chemical reaction plus the absorbed nanomaterial which is from the lubricant additive itself is generated on the worn surfaces.

**Acknowledgments:** The present work was financially supported by the Scientific and Technological Research Program of Chongqing Municipal Education Commission (Grant Nos. KJ1601203, KJ15012005) and the Research Funds for the Yangtze Normal University (Grant Nos. 2016XJQN31, 2017KYQD41).

**Author Contributions:** Hongmei Xie and Bin Jiang carried out the design and drafted the manuscript. Xingyu Hu and Hongli Guo prepared the samples and carried out the tribo-tests. Cheng Peng and Fusheng Pan commented on the results and revised the manuscript. All authors read and approved the final version of the manuscript.

**Conflicts of Interest:** The authors declare that they have no competing interests.

#### References

1. Sunil, B.R.; Ganesh, K.V.; Pavan, P.; Vadapalli, G.; Swarnalatha, C.; Swapna, P.; Bindukumar, P.; Reddy, G.P.K. Effect of aluminum content on machining characteristics of AZ31 and AZ91 magnesium alloys during drilling. *J. Magnes. Alloys* **2016**, *4*, 15–21. [[CrossRef](#)]
2. Grubac, Z.; Metikos-Hukovic, M.; Roncevic, I.S.; Petravic, M.; Peter, R. Functionalization of Biodegradable Magnesium Alloy Implants with Alkylphosphonate Self-Assembled Films. *Mater. Sci. Eng. C* **2013**, *33*, 2152–2158. [[CrossRef](#)] [[PubMed](#)]
3. Tang, C.P.; Liu, W.H.; Chen, Y.Q.; Liu, X.; Deng, Y.L. Effects of thermal treatment on microstructure and mechanical properties of a Mg-Gd-based alloy plate. *Mater. Sci. Eng. A* **2016**, *659*, 63–75. [[CrossRef](#)]
4. Khramov, A.N.; Balbyshev, V.N.; Kasten, L.S.; Mantz, R.A. Sol–Gel Coatings with Phosphonate Functionalities for Surface Modification of Magnesium Alloys. *Thin Solid Films* **2006**, *514*, 174–181. [[CrossRef](#)]

5. Lu, X.; Feng, X.; Zuo, Y.; Zheng, C.; Lu, S.; Xu, L. Evaluation of the micro-arc oxidation treatment effect on the protective performance of a Mg-rich epoxy coating on AZ91D magnesium alloy. *Surf. Coat. Technol.* **2015**, *270*, 227–235. [[CrossRef](#)]
6. Kavyani, M.; Ebrahimi, G.R.; Sanjari, M.; Haghshenas, M. Texture evaluation in warm deformation of an extruded Mg–6Al–3Zn alloy. *J. Magnes. Alloys* **2016**, *4*, 89–98. [[CrossRef](#)]
7. Espinosa, T.; Jiménez, A.E.; Martínez-Nicolás, G.; Sanes, J.; Bermúdez, M.D. Abrasion Resistance of Magnesium Alloys with Surface Films Generated from Phosphonate Imidazolium Ionic Liquids. *Appl. Surf. Sci.* **2014**, *320*, 267–273. [[CrossRef](#)]
8. Zhang, H.; Cheng, W.; Fan, J.; Xu, B.; Dong, H. Improved mechanical properties of AZ31 magnesium alloy sheets by repeated cold rolling and annealing using a small pass reduction. *Mater. Sci. Eng. A* **2015**, *637*, 243–250. [[CrossRef](#)]
9. Prakash, K.S.; Balasundar, P.; Nagaraja, S.; Gopal, P.M.; Kavimani, V. Mechanical and wear behaviour of Mg–SiC–Gr hybrid composites. *J. Magnes. Alloys* **2016**, *4*, 197–206. [[CrossRef](#)]
10. Jiménez, A.E.; Rossi, A.; Fantauzzi, M.; Espinosa, T.; Arias-Pardilla, J.; Martínez-Nicolás, G.; Bermúdez, M.D. Surface Coating from Phosphonate Ionic Liquid Electrolyte for the Enhancement of the Tribological Performance of Magnesium Alloy. *ACS Appl. Mater. Interface* **2015**, *11*, 10337–10347. [[CrossRef](#)] [[PubMed](#)]
11. Xie, H.M.; Jiang, B.; Wang, Q.H.; Xia, X.S.; Pan, F.S. Effects of combined additions of SiO<sub>2</sub> and MoS<sub>2</sub> nanoparticles as lubricant additive on the tribological properties of AZ31 magnesium alloy. *Sci. China Technol. Sci.* **2016**, *59*, 689–698. [[CrossRef](#)]
12. Dennis, J.E.S.; Jin, K.; John, V.T.; Pesika, N.S. Carbon microspheres as ball bearings in aqueous-based lubrication. *ACS Appl. Mater. Interface* **2011**, *3*, 2215–2218. [[CrossRef](#)] [[PubMed](#)]
13. Gu, K.C.; Chen, B.S.; Wang, X.M.; Wang, J.; Fang, J.H.; Wu, J.; Yang, X. Preparation, Friction, and Wear Behaviors of Cerium-Doped Anatase Nanophases in Rapeseed Oil. *Ind. Eng. Chem. Res.* **2014**, *53*, 6249–6254. [[CrossRef](#)]
14. Huang, W.J.; Du, C.H.; Li, Z.F.; Liu, M.; Liu, W.M. Tribological characteristics of magnesium alloy using N-containing compounds as lubricating additives during sliding. *Wear* **2006**, *260*, 140–148. [[CrossRef](#)]
15. Huang, W.J.; Fu, Y.; Wang, J.; Li, Z.F.; Liu, M. Effect of chemical structure of borates on the tribological characteristics of magnesium alloy during sliding. *Tribol. Int.* **2005**, *38*, 775–780. [[CrossRef](#)]
16. Xia, Y.Q.; Jia, Z.F.; Jia, J.H. *Advanced Tribology*; Springer: Berlin/Heidelberg, Germany, 2010.
17. Yan, L.; Yue, W.; Wang, C.; Wei, D.; Xu, B. Comparing tribological behaviors of sulfur- and phosphorus-free organomolybdenum additive with ZDDP and MoDTC. *Tribol. Int.* **2012**, *53*, 150–158. [[CrossRef](#)]
18. Li, Z.P.; Li, X.F.; Zhang, Y.W.; Ren, T.H.; Zhao, Y.D.; Zeng, X.Q.; Heide, E. Tribological study of a highly hydrolytically stable phenylboronic acid ester containing benzothiazolyl in mineral oil. *Appl. Surf. Sci.* **2014**, *308*, 91–99. [[CrossRef](#)]
19. Cai, M.; Liang, Y.; Zhou, F.; Liu, W. Tribological properties of novel imidazolium ionic liquids bearing benzotriazole group as the antiwear/anticorrosion additive in poly(ethylene glycol) and polyurea grease for steel/steel contacts. *ACS Appl. Mater. Interfaces* **2011**, *3*, 4580–4592. [[CrossRef](#)] [[PubMed](#)]
20. Liu, Y.D.; Wang, C.B.; Yuan, J.J.; Liu, J.J. Investigation on anti-wear properties of sulfide layer on bearing steel lubricated by oil-containing FeS particles. *Surf. Coat. Technol.* **2010**, *205*, 470–474. [[CrossRef](#)]
21. Flores-Castañeda, M.; Camps, E.; Camacho-López, M.; Muhl, S.; Garcia, E.; Figueroa, M. Bismuth nanoparticles synthesized by laser ablation in lubricant oils for tribological tests. *J. Alloys Compd.* **2014**, *643*, 67–70. [[CrossRef](#)]
22. Sayuti, M.; Sarhan, A.A.; Hamdi, M. An investigation of optimum SiO<sub>2</sub> nanolubrication parameters in end milling of aerospace Al6061-T6 alloy. *Int. J. Adv. Manuf. Technol.* **2013**, *67*, 833–849. [[CrossRef](#)]
23. Sayuti, M.; Erh, O.M.; Sarhan, A.A.D.; Hamdi, M. Investigation on the morphology of the machined surface in end milling of aerospace AL6061-T6 for novel uses of SiO<sub>2</sub> nanolubrication system. *J. Clean. Prod.* **2014**, *66*, 655–663. [[CrossRef](#)]
24. Hu, K.H.; Liu, M.; Wang, Q.J.; Xu, Y.F.; Schraube, S.; Hu, X.G. Tribological properties of molybdenum disulfide nanosheets by monolayer restacking process as additive in liquid paraffin. *Tribol. Int.* **2009**, *42*, 33–39. [[CrossRef](#)]
25. Kogovšek, J.; Remškar, M.; Mrzel, A.; Kalin, M. Influence of surface roughness and running-in on the lubrication of steel surfaces with oil containing MoS<sub>2</sub> nanotubes in all lubrication regimes. *Tribol. Int.* **2013**, *61*, 40–47. [[CrossRef](#)]
26. Mosleh, M.; Atnafu, N.D.; Belk, J.H.; Nobles, O.M. Modification of sheet metal forming fluids with dispersed nanoparticles for improved lubrication. *Wear* **2009**, *267*, 1220–1225. [[CrossRef](#)]

27. Kalin, M.; Kogovšek, J.; Kovač, J.; Remškar, M. The Formation of Tribofilms of MoS<sub>2</sub> Nanotubes on Steel and DLC-Coated Surfaces. *Tribol. Lett.* **2014**, *55*, 381–391. [[CrossRef](#)]
28. Kogovšek, J.; Remškar, M.; Kalin, M. Lubrication of DLC-coated surfaces with MoS<sub>2</sub> nanotubes in all lubrication regimes: Surface roughness and running-in effects. *Wear* **2013**, *303*, 361–370. [[CrossRef](#)]
29. Xie, H.M.; Jiang, B.; He, J.J.; Xia, X.S.; Pan, F.S. Lubrication performance of MoS<sub>2</sub> and SiO<sub>2</sub> nanoparticles as lubricant additives in magnesium alloy-steel contacts. *Tribol. Int.* **2016**, *93*, 63–70. [[CrossRef](#)]
30. Podgornik, B.; Kocijan, A.; Kocijan, A.; Donik, C. Tribological behaviour and lubrication performance of hexagonal boron nitride (h-BN) as a replacement for graphite in aluminium forming. *Tribol. Int.* **2015**, *81*, 267–275. [[CrossRef](#)]
31. Zhang, L.L.; Pu, J.B.; Wang, L.; Xue, Q.J. Synergistic effect of hybrid carbon nanotube-graphene oxide as nanoadditive enhancing the frictional properties of ionic liquids in high vacuum. *ACS Appl. Mater. Interface* **2015**, *7*, 8592–8600. [[CrossRef](#)] [[PubMed](#)]
32. Cizaire, L.; Vacher, B.; Le-Mogne, T.; Martin, J.M.; Rapoport, L.; Margolin, A.; Tenne, R. Mechanisms of ultra-low friction by hollow inorganic fullerene-like MoS<sub>2</sub> nanoparticles. *Surf. Coat. Technol.* **2002**, *160*, 282–287. [[CrossRef](#)]
33. Chacko, P.K.; Perikinalil, K.R.; Manu, V.T. Evaluation of the Tribological and Thermo-physical Properties of Coconut Oil Added with MoS<sub>2</sub> Nanoparticles at Elevated Temperatures. *Wear* **2015**, *330–331*, 288–308.
34. Wu, L.L.; Zhang, Y.J.; Yang, G.B.; Zhang, S.M.; Yu, L.G.; Zhang, P.Y. Tribological properties of oleic acid-modified zinc oxide nanoparticles as the lubricant additive in poly-alpha olefin and diisooctyl sebacate base oils. *RSC Adv.* **2016**, *6*, 69836–69844. [[CrossRef](#)]
35. Rapoport, L.; Leshchinsky, V.; Lapsker, I.; Volovik, Y.; Nepomnyashchy, O.; Lvovsky, M.; Popovitz-Biro, R.; Feldman, Y.; Tenne, R. Tribological properties of WS<sub>2</sub> nanoparticles under mixed lubrication. *Wear* **2003**, *255*, 785–793. [[CrossRef](#)]
36. Marco, D.; Nadja, S.; Francesco, Z. Stability, Dynamics, and Lubrication of MoS<sub>2</sub> Platelets and Nanotubes. *Langmuir* **2012**, *28*, 7393–7400.
37. Cahangirov, S.; Ataca, C.; Topsakal, M.; Sahin, H.; Ciraci, S. Frictional figures of merit for single layered nanostructures. *Phys. Rev. Lett.* **2014**, *108*, 126103–126108. [[CrossRef](#)] [[PubMed](#)]
38. Giacomo, L.; Elisa, M.; Tomas, P.; Maria, C.R. First principles comparative study on the interlayer adhesion and shear strength of transition-metal dichalcogenides and graphene. *Phys. Rev. B* **2015**, *92*, 173–174.
39. Qu, J.; Bansal, D.G.; Yu, B.; Howe, J.Y.; Luo, H.M.; Dai, S.; Li, H.Q.; Blau, P.J.; Bunting, B.G.; Mordukhovich, G.; et al. Antiwear Performance and Mechanism of an Oil-Miscible Ionic Liquid as a Lubricant Additive. *ACS Appl. Mater. Interface* **2012**, *4*, 997–1002. [[CrossRef](#)] [[PubMed](#)]
40. Sia, S.Y.; Bassyony, E.Z.; Sarhan, A.A.D. Development of SiO<sub>2</sub> nanolubrication system to be used in sliding bearings. *Int. J. Adv. Manuf. Technol.* **2014**, *71*, 1277–1284. [[CrossRef](#)]
41. Tannous, J.; Dassenoy, F.; Lahouij, I.; Le Mogne, T.; Vacher, B.; Bruhács, A.; Tremel, W. Understanding the tribochemical mechanisms of IF-MoS<sub>2</sub> nanoparticles under boundary lubrication. *Tribol. Lett.* **2011**, *41*, 55–64. [[CrossRef](#)]
42. Koroteev, V.O.; Bulusheva, L.G.; Okotrub, A.V.; Yudanov, N.F.; Vyalikh, D.V. Formation of MoS<sub>2</sub> nanoparticles on the surface of reduced graphite oxide. *Phys. Status Solidi B* **2011**, *248*, 2740–2743. [[CrossRef](#)]
43. Li, X.; Cao, Z.; Zhang, Z.; Dang, H. Surface-modification in situ of nano-SiO<sub>2</sub> and its structure and tribological properties. *Appl. Surf. Sci.* **2006**, *252*, 7856–7861. [[CrossRef](#)]
44. Levita, G.; Restuccia, P.; Righi, M.C. Graphene and MoS<sub>2</sub> interacting with water: A comparison by ab initio calculations. *Carbon* **2016**, *107*, 878–884. [[CrossRef](#)]
45. Sia, S.Y.; Sarhan, A.A.D. Morphology investigation of worn bearing surfaces using SiO<sub>2</sub> nanolubrication system. *Int. J. Adv. Manuf. Technol.* **2014**, *70*, 1063–1071. [[CrossRef](#)]
46. Alazemi, A.A.; Etacheri, V.; Dysart, A.D.; Stacke, L.E.; Pol, V.G.; Sadeghi, F. Ultrasoft submicrometer carbon spheres as lubricant additives for friction and wear reduction. *ACS Appl. Mater. Interface* **2015**, *7*, 5514–5521. [[CrossRef](#)] [[PubMed](#)]

